Data acquisition system design for a 1 mm^3 resolution PSAPD-based PET system

Peter D. Olcott, *,Student Member, IEEE,* Frances W. Y. Lau, *Student Member, IEEE,* and Craig S. Levin, *Member, IEEE*

***Abstract*—We are developing an application specific, high resolution 1 mm^3 3-D PET system that comprises two detector panels that are 16 cm x 9.1 cm x 2 cm in dimension with arrays of sandwiched position sensitive avalanche photodiode (PSAPD) detectors. The system will comprise 2240 PSAPD devices per panel with approximately 11,200 channels per detector head. A data acquisition architecture is being designed around dedicated readout ASICs. The readout ASIC, the RENA-3, was developed by NOVA R&D for low noise charge sensitive readout of solid state detectors, with shaping, triggering, and timestamp generation circuitry. Using the RENA-3 evaluation system, two PSAPD devices operated in coincidence achieved a 17.2% global energy resolution, 1 mm^2 spatial resolution, and 11 ns (15.5 ns paired) FWHM coincidence time resolution. A monte-carlo simulation of a PET mammography configuration was used to generate realistic count rates. The realistic count rates were then run through an event based simulation model of the PET mammography system and data acquisition to determine the count rate performance of the architecture. The data acquisition we propose with the RENA-3 ASIC readout should be able to handle a 5 mCi imaged whole body dose in a 160 cm tall woman recoding 75% of the events with a 100 keV low energy threshold.**

I. Introduction

SOLID state photodiode and avalanche photodiode scintillation detectors allow for high spatial 3-D detection of interactions resulting from annihilation photons from positron decay. This has been made possible by the development of a large area position sensitive avalanche photodiodes (PSAPD) that can be sandwiched into 3-D detector geometries [1], [2]. The PSAPD has a small active area and significantly lower gain than corresponding photomultiplier (PMT) detectors. The lower gain prevents the reduction in the number of active channels through extensive multiplexing of the electronic readout. Therefore, the readout electronics for a non-multiplexed PSAPD based 1 mm^3 3-D PET detector will require thousands of electronic readout channels and dedicated ASICs are required to meet the density requirements.

II. Methods and Materials

To evaluate the data acquisition architecture, we performed measurements on a small scale data acquisition evaluation system, simulation studies using Monte-carlo physics transport in realistic phantoms, and event based simulation.

P. D. Olcott is with the Department of Bioengineering, Stanford, CA USA e-mail: (pdo@stanford.edu).

F. W. Y. Lau is with the Department of Electrical Engineering, Stanford, CA

C. S. Levin is with the Department of Radiology, Stanford, CA

Manuscript received Nov 26, 2007

A. Breast-dedicated PET System

We are developing a high resolution application specific 1 mm^3 3-D PET system [4] that comprises two panels of 16 cm x 9.1 cm x 2 cm in dimension. The system will comprise 2240 PSAPD devices per panel with approximately 11,200 channels per detector head (see Fig. 4). In the first phase, we are designing a readout board with 25 RENA-3 ASICS and high density connectors for 800 channels. This will read out a 6.5 mm x 16 cm x 2 cm cassette of the dual panel PET detector. Each layer of the cassette will have an array of 2 x 16 PSAPD devices. Each PSAPD device has an active area of 8 mm x 8 mm coupled to a 8x 8 array of 1 mm x 1 mm x 1 mm LSO crystals. There are 5 layers per cassette (see Fig. 4), and 14 cassettes are stacked to form a panel.

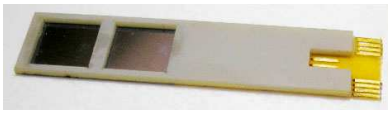

(a) PSAPD-Flex module with Aluminum-Nitride frame

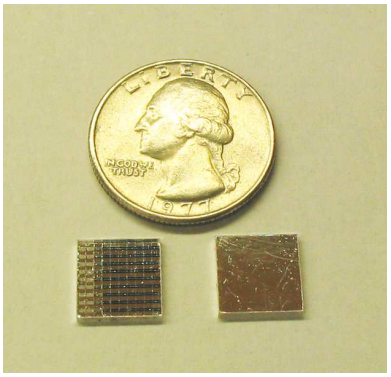

(b) Twp 8x8 arrays of $1mm^3$ LSO crystals with VM2000 Reflector showing the front and back of the arrays

Fig. 1. The LSO-PSAPD 3-D scintillation detector

1) LSO-PSAPD Scintillation Detectors: The scintillation detector consists of two large area, high gain, position sensitive avalanche photodiodes (PSAPDs) [1] glued to a Kapton flex circuit (see Fig. 1(a)). On top of the Kapton flex is a two-piece aluminum-nitride frame. Fabricated crystal arrays are placed and aligned inside the frame and fastened with a melt-mount optical grease (see Fig. 1(b)).

2) Intermediate FLEX interconnect: The PSAPD-FLEX-FRAME devices are placed inside a sensor registration card

1-4244-0923-3/07/$25.00 ©2007 IEEE.

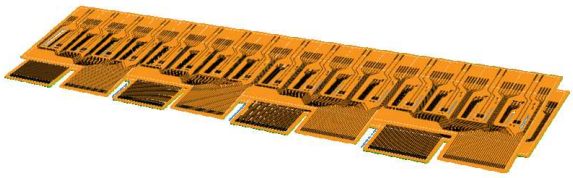

Fig. 2. Intermediate FLEX is used to make connection from the PSAPD Flex to the discrete readout board. Connection between the PSAPD-FLEX and the intermediate flex with be made with solder connections.

(see Fig. 4(b)). Five sensor registration cards will be stacked to form a cassette. The intermediate flex (see Fig. 2) is used to connect the sensor registration card to the PCB (printed circuit board) that houses the discrete components and the readout ASICS. The intermediate flex also separates the high voltage and low voltage connections of the PSAPD so that standard Flex PCB connectors (not requiring HV protection) can be used to connect to the PCB.

3) Readout Cassette: The readout cassette consists of 5 layers of sensor registration cards holding the 16x2 (32) PSAPD-FLEX-FRAME devices (see Fig. 1) connected by an intermediate flex (see Fig. 2) to a discrete readout PCB (see Fig. 3). The discrete board contains all the resistors, capacitors, and HV networks required to couple the analog signals to the readout ASICS. A second readout PCB is directly mounted above the discrete board and contains all the readout ASICS. The analog signals run along the discrete PCB board, travel up vertical connections, and connect to arrays of readout ASICs. The output of the readout ASICs travels out through a vertical connector to an ADC-FPGA readout board. A backplane PCB connects all the ADC-FPGA boards and provides power, buffering, and a high speed optical link to a readout PC.

TABLE I
COMPONENTS OF THE BREAST-DEDICATED PET SYSTEM

PSAPDs per layer	32
Layers per Cassette	5
Cassettes per head	14
Number of panels	2
Total number of PSAPDs	4480
Channels per PSAPD	22400
Dimensions of panel	16 x 9.1 cm x 2 cm

4) LSO-PSAPD Detector Panel: The detector panels is made up of 14 stacked cassettes (see Fig. 4). Tungsten shielding is placed around the detector panels to reduce out of field of view (FOV) activity from saturating the panels. Space has been provided to bring heat out through the sides of the cassettes. Thermal regulation of the PSAPD detectors will be needed to ensure gain and performance stability.

5) RENA-3 ASIC: NOVA R&D (Irvine, CA) has fabricated the RENA-3 ASIC [3] for solid state detectors such as Cadmium-Zinc-Telluride(CZT) and avalanche photodiodes. The RENA-3 ASIC has 36 (in which we use 32) channels of preamplifier, Gaussian shaper, trigger, and timestamp circuitry. The preamplifier and shaper were designed for very low noise

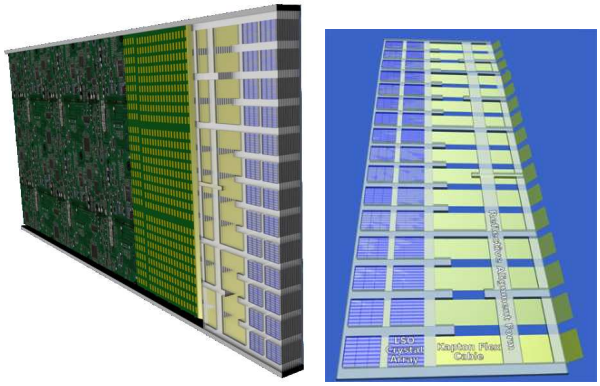

(a) Cutway of a panel of the PET detector (b) Single layer of PSAPD modules

Fig. 4. View of the individual components of a 16 cm x 9.1 cm x 2 cm panel for a PET mammography camera.

readout of semiconductor detectors with a wide range of shaping times and gains. For our application, we used the shortest shaping time of 290 ns. The highly functional RENA-3 ASIC allows for the design of very dense readout electronics with high complexity at reasonable costs.

B. RENA-3 Evaluation

Spatial, energy and time resolution were measured for an RENA-3 Evaluation system comprising a high speed optical link, a FPGA hit processor, a RENA-3 ASIC daughter card, and a PSAPD detector daughter card (see Fig. 7) The PSAPD common channel was connected to the RENA-3 ASIC and operated as the master energy and timing signal. The PSAPD spatial channels are synchronously captured in response to a trigger from the common channel. The RENA-3 ASIC has slow decaying peak-detector to capture the amplitude of a low noise charge sensitive preamplifier-shaper. Also, the RENA-3 ASIC uses a special quadrature sampled 1V 1Mhz sine wave to produce the timing signal. Demodulation of the phase of the timing signal gives accurate timing information for each of the individual interactions on a per channel basis. The RENA-3 operates completely asynchronously, and therefore doesn't generate any noise when not processing events. We are able to determine that the the RENA-3 ASIC should be able to process a PSAPD interaction $12\mu s$ turn-around time, or 83k events per second. Two ceramic packaged PSAPD devices biased at -1710V were placed in coincidence on the daughter card and irradiated with a Na-22 source. 8 mm x 8 mm x 2 mm LSO sheet crystals were used to measure time resolution. An array of 8 x 8 LSO 1 mm x 1 mm x 1mm crystals coupled to both detectors measured spatial resolution and energy resolution. 220pF capacitors were placed across the spatial channels to reduce the dynamic range of the PSAPD signals to prevent saturation of the spatial channel amplifiers. Also, 100 pF of capacitance was used to attenuate some charge across the device to prevent clipping on the common channel.

C. Simulation

Simulation was used to determine the theoretical count rate performance of this data acquisition architecture. The detector

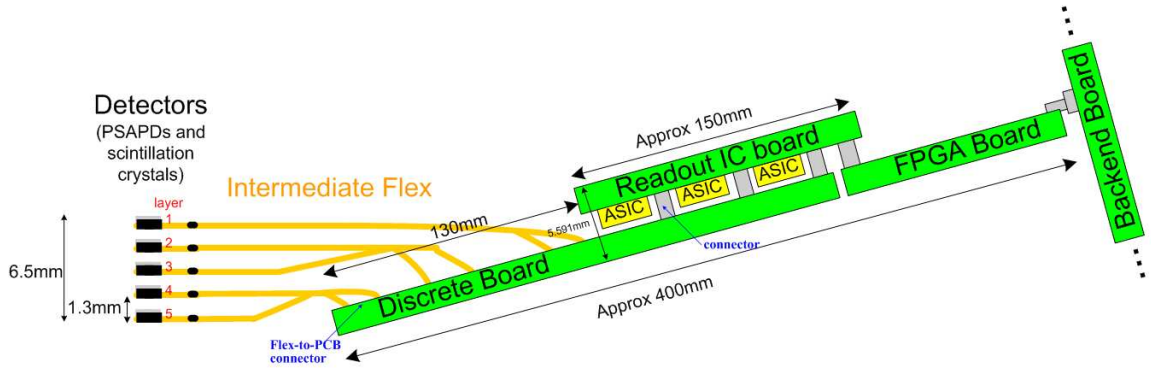

Fig. 3. Block diagram of the readout cassette. The scintillation detectors coupled with intermediate flex connect to the discrete board. A readout ASIC board is connected to the discrete PCB board to an ADC-FPGA board. A backplane PCB board connects all the ADC-FPGA boards and contains high speed optical links to storage PCs.

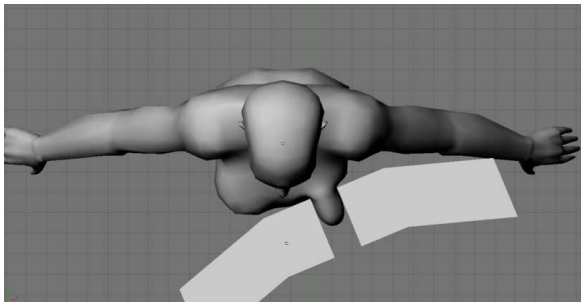

(a) Realistic CAD modeling of a patient and detector placement

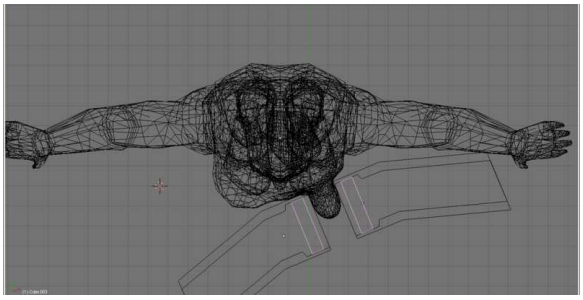

(b) A tungsten shield was placed around the dual panel PET detector

Fig. 5. GRAY can import vectorial representations of phantoms and detectors. Vectorial geometries are easily created and modified using CAD programs such as Blender.

panels were placed in close proximity to the patient so that out of field of view activity would project onto the detector panels.

1) Monte-Carlo Simulation Using GRAY: A realistic phantom with accurate detector placement was modeled using the Blender CAD program. We used GRAY to simulate the high energy photon transport through the model [5]. Also, we are using this CAD model to help design the tungsten shielding (see Fig. 5(b)) of the camera. In our current design, the tungsten shielding is approximately 5 mm thick at the patient chest wall. This was chosen to reduce the high singles rate, but at the same time preserve the FOV of the camera.

2) Data Acquisition Simulation: A timing-accurate event based simulator predicts the saturation performance of a data acquisition. The timing-accurate behavior of the different hardware components can be modeled (see Fig 6(a)). Using a priority-queue, events can be processed in time-sorted order (see. Fig. 6(b)). When two events try to occupy the same piece of hardware, a collision is recorded. By analyzing the collisions, the efficiency of the data acquisition can be determined as a function of count rate. Efficiency is the percentage of hits correctly recorded by the hardware. The overall system sensitivity, S, equals the DAQ efficiency squared, E, times the geometric sensitivity, G, times the intrinsic sensitivity squared, I.

$$S = E^2 \cdot G \cdot I^2 \tag{1}$$

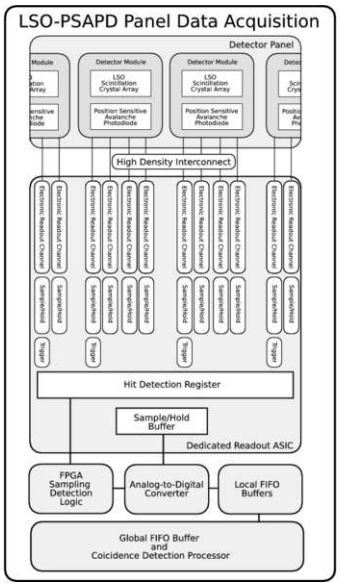

(a) The hardware components of the DAQ and the simulation start with the front-end scintillation crystals, readout ASICS, and the back-end digital storage. The DAQ architecture stores events in list mode for off-line processing.

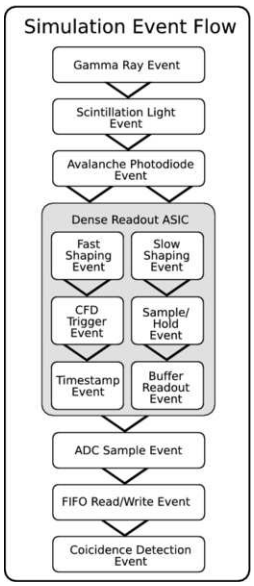

(b) Event based simulation can do timing accurate modeling of all the components of a DAQ.

Fig. 6. Using realistic performance parameters measured from the evaluation system, simulation can provide system level performance which can be used to predict bottlenecks in the design.

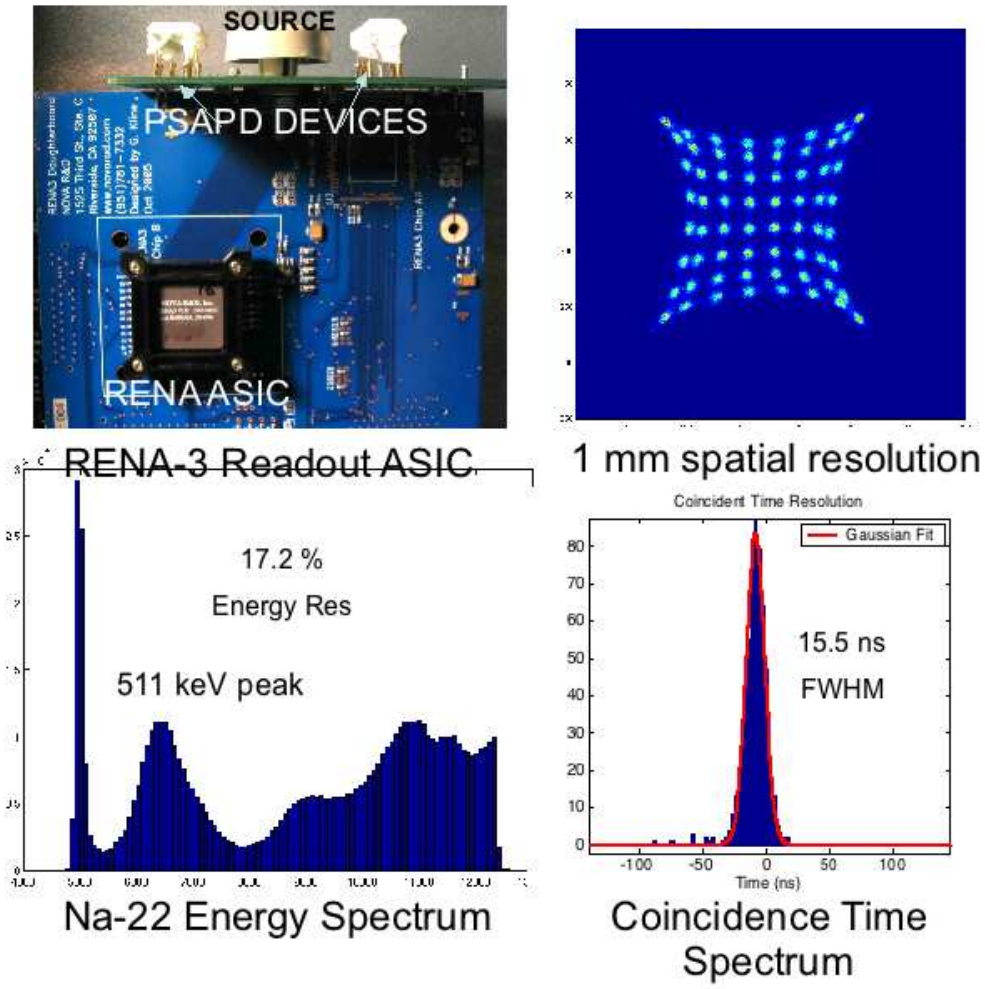

Fig. 7. Two PSAPD devices are setup for a Na-22 coincidence experiment and readout using a RENA-3 data acquisition system. A 8x8 array of 1x1x1 mm^3 crystals are resolved, with excellent global energy (17.2%) spectra and adequate time resolution (15.5 ns FWHM).

III. Results

A. RENA-3 Evaluation

Initial experiments show that the RENA-3 ASIC can resolve an 8 x 8 array of 1 mm x 1 mm x 1mm LSO scintillation crystals with a 17.2% global FWHM energy resolution. Using 8 mm x 8 mm x 2 mm sheet crystals , the RENA-3 ASIC has $\leq$ 11 ns (15.5 ns paired) FWHM time resolution (see Fig. 7). The time resolution performance is limited by the leading edge discriminators.

B. Monte-Carlo Simulation

GRAY is able to generate uniform distributions of positrons inside a vectorial phantom using spatial rejection testing (see Fig. 8). By specifying total dose in the volume, realistic count rates can be generated. Heart activity was added to the whole body phantoms with 3x concentration over background. 5 mm of tungsten shielding at the chest wall and 1.5 cm surrounding the top and bottom were able to significantly reduce the event rate of the panels (see Fig. 9). With adequate shielding, the panel event rate can be reduced from $14x10^6$ events per second to $4x10^6$ events per second.

C. DAQ Simulation

As events are captured by the trigger timestamp circuitry, they are held while the ADC is scheduled to read the event. While the ADC is reading events, the readout ASIC will drop new incoming events. In the data acquisition simulation (see Fig. 11), the efficiency is limited by the dropping of events in the sample-hold of the readout ASIC while it is waiting for ADC conversion. The efficiency of the data acquisition is approximately 75% at 5 mCi of whole body image dose with a event rate of approximately 4.6 millions events per second (see Fig. 12).

D. Discussion

The RENA-3 ASIC has excellent spatial and energy resolution performance with PSAPD devices. Signal processing algorithms are likely to produce significant time resolution improvements, as the RENA-3 evaluation system was not specifically designed for PET. The current time resolution is adequate for low-medium count rate PET applications for application-specific PET or small animal PET systems. We are investigating amplitude dependent correction of the time walk

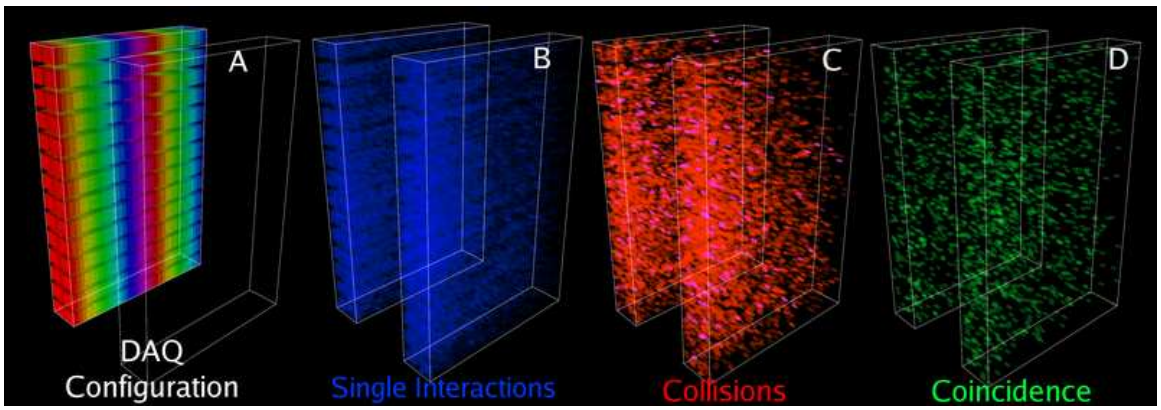

Fig. 11. Visualization of four aspects of the data acquisition. (left) The colors represent the unique encoding of a particular PSAPD to a particular readout chip. The blue boxes correspond to singles. The green boxes correspond to detected coincidences. The red and magenta correspond to collisions. Lost efficiency in the data acquisition is the result of pile-up in the sample-hold of the readout ASIC.

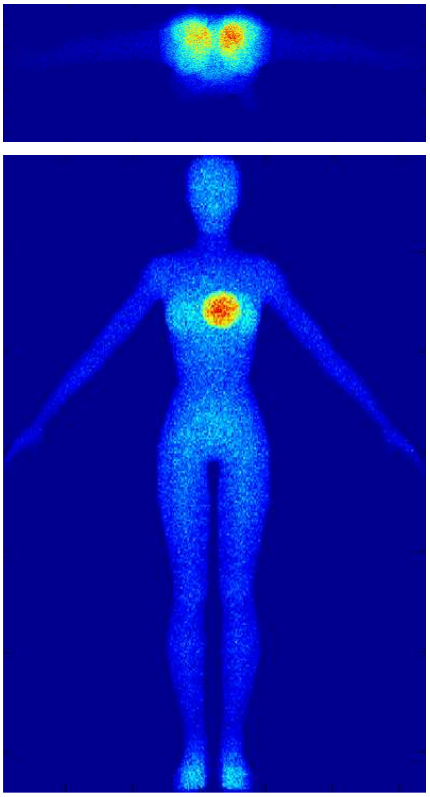

Fig. 8. GRAY uses rejection testing to produce uniform decays within a vectorial volume. Heart activity is also modeled at 3 times the background concentration.

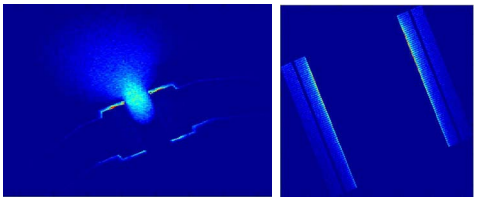

Fig. 9. Approximately $4x10^6$ interactions per second hit the detector panels at 5 mCi of whole body dose (right). The plot on the left records all interactions that lead to interactions in the detector panels. A significant number of interactions are scattered into the detector panels. Good energy resolution will be able to reject most of these events.

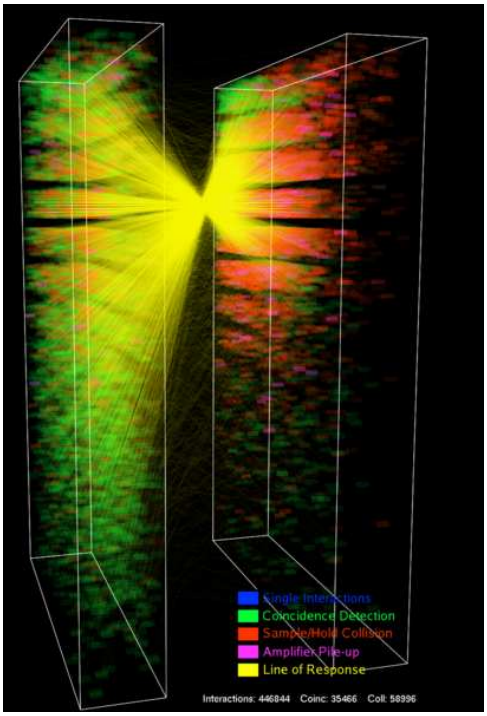

Fig. 10. Visualization of DAQSim for a $100\mu Ci$ point source placed near one of the panels. The green boxes and yellow lines represent detected coincidences. The red and magenta boxes represent collisions. The accumulated area of red collisions represent pileup for the data acquisition system.

from the leading edge discriminator. This is possible since all time stamps, and amplitudes are stored in list mode for offline correction.

IV. Conclusion

We have designed a data acquisition architecture for a 800 channel readout card for very high resolution 3-D PET detectors. We have done initial feasibility on a PET readout ASIC, the RENA-3 that can achieve the necessary power, cost, and performance for a PSAPD breast-dedicated PET

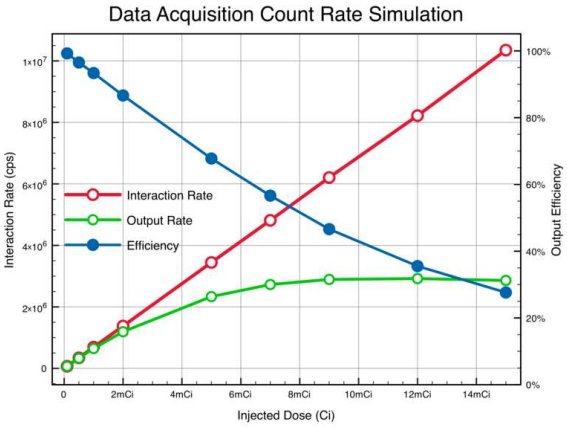

Fig. 12. Simulated whole body doses ranging from 1 mCi to 15 mCi were simulated. The red line gives the singles event rate for the two panels as a function of dose. The green line is the event rate of correctly recorded single events by the data acquisition. The blue line is the efficiency of the data acquisition. At 5 mCi of whole body imaged dose, the data acquisition system has approximately 75% efficiency.

system. A Monte-carlo physics simulation coupled to an event-based hardware simulator verified that our data acquisition architecture is likely to have the count rate performance in the presence of significant out-of-field-of-view activity. This high density readout architecture can also be used for other high channel count solid state PET detectors such as CZT.

ACKNOWLEDGMENT

The authors would like to thank Rick Farrel of RMD, Inc for the ceramic PSAPD devices, Tim Thurston for mechanical design of the system, and all the people at NOVA R&D for help with the RENA-3 ASIC. This work was funded by the NIH, grant R01CA119056, and the California Breast Cancer Research Program, grant 12IB-0092.

REFERENCES

[1] Shah, K.S.; Farrell, R.; Grazioso, R.; Harmon, E.S.; Karplus, E., "Position-sensitive avalanche photodiodes for gamma-ray imaging" Nuclear Science, IEEE Transactions on, Vol.49, Iss.4, Aug 2002 Pages: 1687- 1692

[2] Levin, C.S.; Foudray, A.M.K.; Olcott, P.D.; Habte, F., "Investigation of position sensitive avalanche photodiodes for a new high-resolution PET detector design", *Nuclear Science, IEEE Transactions on*, Vol.51, Iss.3, June 2004 Pages: 805- 810

[3] T.O. Tumer, V.B. Cajipe, M. Clajus, F. Duttweiler, S. Hayakawa, J.L. Matteson, A. Shirley, O. Yossifor. Best results of a CdZnTe pixel detector read out by RENA-2 IC,Presented at the14th International Workshop on Room-Temperature Semiconductor X-Ray and Gamma-Ray Detectors, Rome, Italy (October 2004) and submitted to *IEEE Trans. Nucl. Sci*.

[4] Levin, C.S., "Design of a high-resolution and high-sensitivity scintillation crystal array for PET with nearly complete light collection", *Nuclear Science, IEEE Transactions on*, Vol.49, Iss.5, Oct 2002, Pages: 2236-2243

[5] Olcott, P.D.; Buss, S.R.; Levin, C.S.; Pratx, G.; Sramek, C.K., "GRAY: High Energy Photon Ray Tracer for PET Applications", *Nuclear Science Symposium Conference Record*, 2006. IEEE , vol.4, no., pp.2011-2015, Oct. 29 2006-Nov. 1 2006